



Fine Particulate Matter Exposure and Health Impacts from Indoor Activities

Bhoonah, Rachna; Maury-Micolier, Alice; Jolliet, Olivier; Fantke, Peter

Published in:
Indoor Air

Link to article, DOI:
[10.1155/2023/8857446](https://doi.org/10.1155/2023/8857446)

Publication date:
2023

Document Version
Publisher's PDF, also known as Version of record

[Link back to DTU Orbit](#)

Citation (APA):
Bhoonah, R., Maury-Micolier, A., Jolliet, O., & Fantke, P. (2023). Fine Particulate Matter Exposure and Health Impacts from Indoor Activities. *Indoor Air*, 2023, Article 8857446. <https://doi.org/10.1155/2023/8857446>

General rights

Copyright and moral rights for the publications made accessible in the public portal are retained by the authors and/or other copyright owners and it is a condition of accessing publications that users recognise and abide by the legal requirements associated with these rights.

- Users may download and print one copy of any publication from the public portal for the purpose of private study or research.
- You may not further distribute the material or use it for any profit-making activity or commercial gain
- You may freely distribute the URL identifying the publication in the public portal

If you believe that this document breaches copyright please contact us providing details, and we will remove access to the work immediately and investigate your claim.

Research Article

Fine Particulate Matter Exposure and Health Impacts from Indoor Activities

Rachna Bhoonah ^{1,2}, Alice Maury-Micolier ³, Olivier Jolliet ^{4,5} and Peter Fantke ⁴

¹Mines Paris-PSL, CES-Center for Energy Efficiency of Systems, 60 Bd St Michel, 75006 Paris, France

²UMR ECOSYS, INRAE, AgroParisTech, Université Paris-Saclay, 91120 Palaiseau, France

³Octopus Lab, 237 rue du Ballon, 59110 La Madeleine, France

⁴Quantitative Sustainability Assessment, Department of Environmental and Resource Engineering, Technical University of Denmark, Bygningstorvet 115, 2800 Kongens Lyngby, Denmark

⁵Environmental Health Sciences, School of Public Health, University of Michigan, Ann Arbor, MI 48109, USA

Correspondence should be addressed to Rachna Bhoonah; rachna.bhoonah@minesparis.psl.eu and Peter Fantke; pefan@dtu.dk

Received 14 July 2023; Revised 29 September 2023; Accepted 29 October 2023; Published 21 November 2023

Academic Editor: Faming Wang

Copyright © 2023 Rachna Bhoonah et al. This is an open access article distributed under the Creative Commons Attribution License, which permits unrestricted use, distribution, and reproduction in any medium, provided the original work is properly cited.

Exposure to fine particulate matter (PM_{2.5}) is an important contributor to global human disease burden, particularly indoors where people spend the majority of their time and exposure is highest. We propose a framework linking indoor PM_{2.5} emissions from human activities to exposure and health impacts, expressed in Disability-Adjusted Life Years (DALY). Derived dynamic indoor PM_{2.5} concentrations—capturing temporal variations through different window-opening scenarios and air renewal rates—are used to estimate uncertainty for a parametric model (up to a factor of 114). Intake fractions (fraction of emitted substance taken in ($\mu\text{g}_{\text{intake}}/\mu\text{g}_{\text{emitted}}$)), effect factors ($\mu\text{DALY}/\mu\text{g}_{\text{intake}}$), related impact characterisation factors (health impact per unit mass emitted ($\mu\text{DALY}/\mu\text{g}_{\text{emitted}}$)), and impact scores (health impact per hour activity ($\mu\text{DALY}/\text{h}_{\text{activity}}$)) are provided for 19 one-hour indoor activities and can be flexibly scaled to real activity durations. Indoor concentrations exceeded recommended World Health Organization (WHO) limits for all activities at low ventilation rates. Per person, 98 to 119 $\mu\text{DALY}/\text{h}_{\text{activity}}$ (52 to 63 $\text{minutes}_{\text{lost}}/\text{h}_{\text{activity}}$) was associated with traditional fuel cook stoves, with high air renewal rates (3 and 14h^{-1}). The burning of candles, at low air renewal rates of 0.2 to 0.6h^{-1} , results in 7 to 11 $\mu\text{DALY}/\text{h}_{\text{activity}}$ (4 to 11 $\text{minutes}_{\text{lost}}/\text{h}_{\text{activity}}$). Derived impact scores and characterisation factors serve as a starting point for integrating indoor PM_{2.5} emissions and exposure into life cycle impact and public health assessments.

1. Introduction

Ambient and household fine particulate matter (PM_{2.5}) pollution is one of the major global health risk factors, representing 120 million and 92 million Disability-Adjusted Life Years (DALYs) each in 2019 (4.7% and 3.6% of total DALYs) [1]. Serious health outcomes are associated with PM_{2.5} exposure, including chronic obstructive diseases (COPD), ischemic heart disease (IHD), stroke and lung cancer (LC) for adults, and acute lower respiratory diseases (ALRI) for children who are still in the developmental stage (<5 years) [2, 3]. Indoor environments, where people spend

a large fraction of their time, are particularly important to study: 83% to 90% of exposure occurs indoors [4]. Since buildings have relatively small, enclosed volumes, indoor air concentrations can be particularly high as compared to ambient levels. For instance, PM_{2.5} air concentrations were higher than the World Health Organization's (WHO) annual guideline values in schools and kindergartens by a factor of 4 to 15 [5–7]. According to these guidelines, annual exposures should remain below $5\mu\text{g}/\text{m}^3$, and 24 hour exposures can exceed $15\mu\text{g}/\text{m}^3$ for no more than 3 to 4 days per year [8]. Inhabitants of rural areas, especially in developing countries, are particularly at risk due to the

wide usage of solid fuel combustion indoors for cooking or heating [9–11].

Indoor $PM_{2.5}$ concentrations depend on outdoor pollution levels, penetrating through unfiltered ventilation, indoor primary $PM_{2.5}$ emissions from human activities, and chemical reactions between chemicals emitted indoors, such as the oxidation of volatile organic compounds (VOCs), with ozone, nitrate, and hydroxyl radicals, which together can form secondary PM [12]. Various studies have measured primary $PM_{2.5}$ emission rates, indoor concentrations, and particle size distributions [13–21] for different activities. While fuel stoves are recognised as strong indoor $PM_{2.5}$ sources and linked to premature mortality in developing countries, cooking (especially frying and grilling) and candle burning were also identified as important sources. Occupant contributions to indoor $PM_{2.5}$ from the shedding of skin and cloth fibres or the resuspension of particles during activities [22–26] have also been measured and are highly dependent on dust coverage and, ultimately, occupant behaviour (e.g. frequency of cleaning or presence in dusty environments). Indoor concentrations are affected by air changes per hour (ACH), the presence of filters for mechanical ventilation, and the size and orientation of windows for natural ventilation.

Human health impacts of products from outdoor $PM_{2.5}$ emissions can be calculated using life cycle assessment (LCA), a tool used to evaluate the environmental performance of products and technologies over their life cycles, considering different impact categories. The UNEP/SETAC Life Cycle Initiative identified the $PM_{2.5}$ impact category as one of the categories requiring refinements [3]. While indoor emissions of chemicals are characterized in terms of human exposure and effects using other models, such as USEtox [27], there is a need for representative indoor archetypes treating indoor sources of $PM_{2.5}$ and related occupant exposures and health impacts.

Archetypes have been defined by Fantke et al. [4] according to parameters identified by Hodas et al. [28], including air renewal rates and occupancy. Parametric models coupled with these indoor archetypes can provide average $PM_{2.5}$ concentrations and intake fractions (mass taken in per unit mass emitted) [4], but usually do not capture temporal variations in emission or ventilation rates. Dynamic simulations, using airflow simulation tools such as CONTAM (used by INCA-Indoor [29]) or COMIS, can provide full concentration/exposure profiles that can be coupled with effect factors to calculate health impacts. There is still, however, a need for defining emission scenarios linked to indoor sources and their emission rates. In addition, factors linking emissions, exposure, and health effects to particular indoor activities are missing in LCA literature. To address this gap, our study is aimed at proposing a framework for characterising human exposure to $PM_{2.5}$ and related health impacts associated with common indoor activities and their emissions. To achieve this aim, we will address the following three specific objectives:

- (1) Propose a framework for linking human indoor activities to primary $PM_{2.5}$ emissions, exposure, effects, and health damage based on a dynamic modelling approach

- (2) Calculate dynamic indoor $PM_{2.5}$ concentrations and derive a parameterised exposure and effect model for integration in life cycle impact assessment
- (3) Provide a set of impact characterisation factors for different reference indoor activities under different natural ventilation scenarios

Resuspension and secondary $PM_{2.5}$ are not within the scope of this study, since they depend on dust coverage and the presence of precursors such as VOCs, which are not currently treated by the dynamic model.

2. Methods

2.1. Overall Followed Source-to-Damage Approach. The pollutant pathway from emission to impact is modelled using the framework recommended in global consensus-building efforts for $PM_{2.5}$ exposure and effects [3, 30], adapted to indoor contexts (Figure 1). The functional unit is defined as one hour of activity.

Indoor $PM_{2.5}$ concentrations (C_{in} ($\mu\text{g}/\text{m}^3$)) are simulated with INCA-Indoor, considering (1) indoor emission rates of different activities ($\dot{m}_{\text{emitted in, avg}}$ ($\mu\text{g}_{\text{emitted}}/\text{h}_{\text{activity}}$)) obtained from studies, (2) the penetration from outdoors with natural ventilation ($\dot{m}_{\text{penetration, avg}}$ ($\mu\text{g}/\text{h}$)) (equation (5)), and (3) air renewal rates (h^{-1}). These are compared to a parametric model's results, using one hour as the reference activity duration under multiple given air change rates (ACH (h^{-1})). Using a fate factor (FF (h)) or the dynamic fate model INCA-Indoor, we determine the evolution of the indoor $PM_{2.5}$ concentrations and the resulting time-integrated mass inside the room air. These masses are then multiplied by the exposure rates (h^{-1}) to yield indoor $PM_{2.5}$ intake fractions (iF ($\mu\text{g}_{\text{intake}}/\mu\text{g}_{\text{emitted}}$)) (equation (2)). These iFs are multiplied by effect factors (EF ($\mu\text{DALY}/\mu\text{g}_{\text{intake}}$)) to obtain the characterisation factors (CF ($\mu\text{DALY}/\mu\text{g}_{\text{emitted}}$)), i.e., the impact per unit of $PM_{2.5}$ emitted. Impact scores (IS ($\mu\text{DALY}/\text{h}_{\text{activity}}$)) for one person are then calculated as the product of the cumulative indoor emission ($m_{\text{emitted in}}$ ($\mu\text{g}_{\text{emitted}}$)) and CFs. This can therefore be expressed as

$$IS_{\text{activity}} = EF \times iF \times m_{\text{emitted in}} = CF \times m_{\text{emitted in}}, \quad (1)$$

with

$$iF = \frac{\int_{t=0}^{\infty} BR \times POP \times C_{\text{in, inc}} dt}{m_{\text{emitted in}}}, \quad (2)$$

where POP (cap) is the number of occupants, BR is the breathing rate of an occupant ($\text{m}^3/\text{cap}/\text{h}$), and $C_{\text{in, inc}}(t)$ is the increase in indoor $PM_{2.5}$ concentration due to the activity-related emissions ($\mu\text{g}/\text{m}^3$) integrated up to infinity (in practice, up to the time required to entirely evacuate the particles emitted by the activity). It is given by the difference between indoor concentration with activity (C_{in} , in $\mu\text{g}/\text{m}^3$) and without (C_{base} , in $\mu\text{g}/\text{m}^3$).

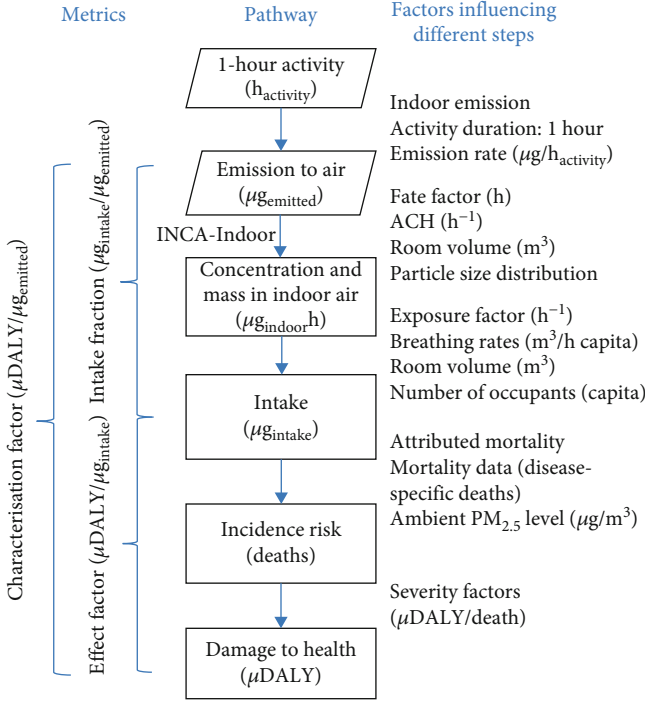


FIGURE 1: Framework for the calculation of activity impact scores from $PM_{2.5}$ emission rates.

The effect factor depends on the average effective indoor concentration (\bar{C}_{in}) and the annual average ambient concentration of the region ($\bar{C}_{out,r}$) [31, 32].

$$\begin{aligned}
 EF(\bar{C}_{in}) &= \frac{dM_{PM_{2.5}}}{dI_{in}} \times SF_{i,r} \\
 &= \frac{(RR_i(\bar{C}_{in} + \Delta C_{in}) - RR_i(\bar{C}_{in})) \times (M_{i,r}/(RR_i(\bar{C}_{out,r}) \times POP_r)) \times SF_{i,r}}{\Delta \bar{C}_{in} \times BR_{yr}}
 \end{aligned} \quad (3)$$

where $RR_i(-)$ is the relative risk of developing disease i from exposure to \bar{C}_{in} (see Fantke et al., [32]), $\Delta \bar{C}_{in}$ ($\mu g/m^3$) is the increment on the exposure-response curve, $M_{i,r}$ (deaths/year) is the annual mortality in region r due to disease i , POP_r (cap) is the population of the region, $SF_{i,r}$ (DALY/death) is the severity factor specific to the region and disease, and BR_{yr} ($m^3/year$) is the breathing rate. The effect factor depends on exposure concentrations and can hence be different for activities with different emission rates.

The EF depends on the average effective indoor concentration (\bar{C}_{in}). This can be calculated either by INCA-Indoor or as a comparison calculated using Fantke et al. [4], adapted to consider intake and deposition for outdoor $PM_{2.5}$:

$$\bar{C}_{in} = \frac{(\dot{m}_{emitted,avg} + \dot{m}_{penetration,avg})}{V_{room} \times (ACH_{avg} + DR_{avg} + (BR_{avg} \times POP_{avg})/V_{room})}. \quad (4)$$

$\dot{m}_{penetration,avg}$ ($\mu g/h$) is the average penetration rate of $PM_{2.5}$ from outdoors, defined by

$$\dot{m}_{penetration,avg} = \bar{C}_{out} \times V_{room} \times ACH_{avg}. \quad (5)$$

\bar{C}_{out} ($\mu g/m^3$) is the average outdoor $PM_{2.5}$ concentration.

2.2. Individual Lifetime Risk. The total individual lifetime risk (\overline{ILR} (DALY/person)) represents the number of life years lost from exposure to $PM_{2.5}$ over a lifetime for each one-hour activity. It is calculated using the following equation.

$$\overline{ILR} = N_{activity} \times IS_{activity}, \quad (6)$$

where $N_{activity}$ is the number of one-hour activities occurring during a lifetime.

2.3. Emission Data. Primary $PM_{2.5}$ emission rates are collected from various studies for 19 activities and are presented in Table 1.

Cook stove emission rates are highest (up to 120 mg/min) and correspond to common practices in certain rural Chinese homes [20]. Model parameters, including reference outdoor $PM_{2.5}$ concentration and air renewal rates, are given in the supporting information SI section S.1.

2.4. Dynamic Indoor $PM_{2.5}$ Concentration Calculation. Dynamic concentrations are simulated using the INCA-Indoor multizone model [29]. The following inputs are necessary for the simulation: (1) building characteristics, including room dimensions, mechanical ventilation rates if any (not considered in this study), window sizes, and layout (modelled with the Pleiades software [35]); (2) dynamic outdoor $PM_{2.5}$ concentrations; (3) meteorological data (temperature, wind speed, and direction); (4) indoor $PM_{2.5}$ emission rates; (5) time and duration of emissions; and (6) particle size distribution. Room volumes of 30 m^3 and 67 m^3 are considered, corresponding to 12 m^2 and 27 m^2 flooring areas, respectively, which are within the range of average bedrooms and kitchens [36–38]. Air flows are simulated with CONTAM based on the opening of windows, infiltration rates under 4 Pa, and meteorological data, considering a constant indoor temperature of 20°C. Any interconnecting door between rooms is assumed to be closed, while infiltrations and airflows from differences between open versus closed windows are explicitly considered. Concentrations are calculated with a time step of 10 minutes as a function of airflow rates, emission rates, outdoor $PM_{2.5}$ concentrations, and deposition rates.

The INCA-Indoor model calculates air PM concentrations based on their size distribution, separated into 27 categories of 0.004 μm to 10 μm . Since particle size distributions are only available for some specific activities, we select a more general indoor distribution, irrespective of the emission source [39]. The distributions are provided in SI section S.3.

Because the dynamic model allows the capture of variations in air renewal rates, scenarios have been defined to evaluate the effect of window opening on concentrations and health impacts for each activity, hence estimating uncertainties of the parametric model. Air change exchange rates (ACH) between indoor and outdoor air are defined according to Fantke et al. [4]. The average ACH for OECD countries is 0.64 ACH [40], while low-end values are around

TABLE 1: Primary PM_{2.5} emission rates for 19 activities.

| Activity | PM _{2.5} emission rate (mg/min) | Reference |
|---|--|-----------------------------|
| Candle burning (low) | 0.04 | Pagels et al. [13] |
| Toasting | 0.11 | He et al. [16] |
| Cooking with electric stove (low) | 0.11 | He et al. [16] |
| Candle burning (medium) | 0.15 | Pagels et al. [13] |
| Incense: aromatic (low) | 0.16 | Lee and Wang [33] |
| Gas stove | 0.24 | He et al. [16] |
| Printer (high) | 0.28 | He et al. [34] |
| Frying (low) | 0.43 | Aquilina and Camilleri [14] |
| Grilling (low) | 0.62 | Aquilina and Camilleri [14] |
| Candle with eucalyptus oil diffusion (high) | 0.91 | He et al. [16] |
| Smoking (passive) | 0.99 | He et al. [16] |
| Cook stove (low) ^a | 1.2 | Du et al. [20] |
| Cooking (high, with burning) | 1.33 | Aquilina and Camilleri [14] |
| Frying (high) | 2.68 | He et al. [16] |
| Grilling (high) | 2.78 | He et al. [16] |
| Coal-heating stove ^d | 3.50 | Li et al. [21] |
| Incense: traditional (high) | 6.21 | Lee and Wang [33] |
| Cook stove (medium) ^b | 7.9 | Shen et al. [18] |
| Cook stove (high) ^c | 120 | Du et al. [20] |

^aFugitive emissions (leakage) from cooking with the burning of coal in an iron stove. ^bFugitive emissions from cooking with the burning of wood in a brick stove. ^cFugitive emissions from cooking with the burning of maize straw in a brick stove. ^dEmission rate (mg/min) calculated from the emission factor (g/kg), as described in SI.

0.2 ACH for airtight buildings [41]. High air change rates are around 3 ACH, and in non-OECD countries, they can reach 14 ACH.

Four standard scenarios are defined: windows always closed with infiltration rates of 0.2 ACH and 0.6 ACH and windows always open with high and very high ventilation rates of 3 ACH and 14 ACH, respectively. The air change rates indicated are 24 hour averages, but air flows vary during the day for natural ventilation due to changes in wind speed and direction, temperature, and pressure. In the remaining six scenarios, windows are open either before, during, or after activity, with high and very high average air renewal rates of 3 ACH and 14 ACH. Since windows are open for a limited duration in the last six scenarios (a minimum of one hour allowed by the model), the ACH can be much higher when open in order to reach the target 24 hour average, but do not exceed a reference comfort speed of 1 m/s [42]. Dynamic ACH are illustrated in SI Figure S2. Very high ventilation rates typically correspond to hot or tropical regions, where cross-ventilation is common. The 10 ventilation scenarios are summarised in SI section S.1.

2.5. Exposure Model Data. The intake fractions for one occupant are calculated using equation (2) for dynamic concentrations using a breathing rate (BR) of 16 m³/d [28] and an exposure duration of 24 hours.

2.6. Effect (IER) Model Data. Global population data are obtained from world population prospects [43], and age-specific global mortality rates, M (deaths/year), for the five disease outcomes are obtained from the GBD Collaborative

Network for 2019 [44]. An annual average ambient PM_{2.5} level of 16 µg/m³, corresponding to an average European city [45], is considered, and average exposure concentrations (\bar{C}_{in} (µg/m³)) are calculated over 24 hours. The calculated effect factor (EF) only corresponds to exposure to one activity and ambient PM_{2.5} concentrations, without considering the occurrence of several activities at the same time.

3. Results and Discussion

3.1. Dynamic Indoor PM_{2.5} Concentrations. Dynamic PM_{2.5} concentrations from four indoor activities in a reference room of 30 m³ with closed windows at 0.6 ACH are presented in Figure 2 over 24 hours, a duration that allows to evacuate most activity-related PM_{2.5} from indoor air. Indoor and outdoor concentrations are dynamic. Indoor concentrations increase after emission and decrease due to evacuation with air renewal. Outdoor concentrations vary independently of the indoor activity, due to the change in outdoor emissions (e.g., fuel burning) or wind speeds.

PM_{2.5} concentration increments are higher for higher emission rates: the use of a coal-heating stove can lead to a peak of 4500 µg/m³, while toasting or cooking on an electric stove leads to a peak of 150 µg/m³. The area under the curve gives the concentration to which occupants are exposed over a given duration (µg·s/m³), which is important to consider in health impact assessment. It is ultimately linked to the decay rate, mainly determined by the air change rate: higher ACH lead to higher decay rates.

24 h average concentrations for the different activities and ventilation scenarios, calculated from results of the

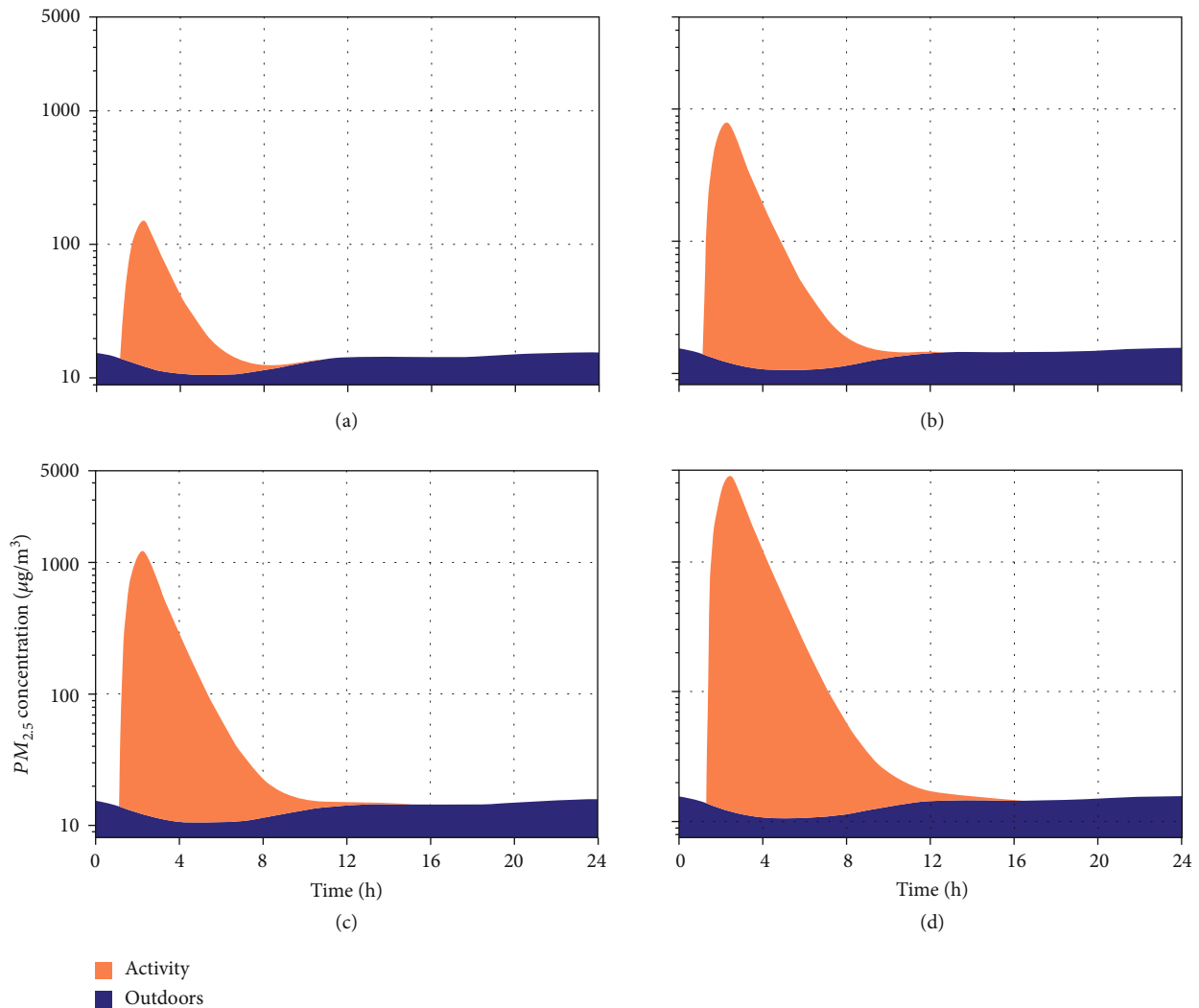


FIGURE 2: Indoor $PM_{2.5}$ concentrations from outdoors (navy) and increment from one-hour activities (orange) over 24 hours: (a) toasting or cooking on an electric stove, (b) grilling (low), (c) smoking or lighting a candle with essential oil diffusion, and (d) coal-heating stove.

dynamic model, are presented in Figure 3 for the room with small volume/high occupancy (HO) of $30\text{ m}^3/\text{occupant}$. Concentrations in the room with higher volume/low occupancy (LO) of $67\text{ m}^3/\text{occupant}$ correspond to the average ventilation rate of 0.6 ACH.

The increment in the larger room is on average 2.5 times lower than that in the smaller room, and the ratio of their volumes is 2.2. The difference can be explained by a higher deposition rate in the larger room due to the larger available surface area. Higher ventilation rates lead to a decrease in concentrations if windows are always open or closed. We note from the other scenarios presented in Figure 3(b) that least concentrations are linked to opening windows during the activity, since ventilation rates during emission are much higher, while opening before the activity does not affect concentrations: they are equal to the closed window scenario. Opening after the activity allows for partial evacuation of substances and hence a slight decrease in concentrations (see SI Figure S2).

3.2. Parametric Model Indoor $PM_{2.5}$ Concentrations. The average $PM_{2.5}$ concentrations over 24 hours are calculated for each activity with the parametric model described by equation (4). Though the parametric model with a mean ACH throughout the day can provide a good estimation of 24 h average indoor air concentrations (e.g., for fixed mechanical ventilation), under certain conditions, the dynamic model is more precise. In most cases, the ACH changes throughout the day according to the opening/closing of windows and meteorological conditions. The latter determines natural air flow rates through openings and infiltration. If variations in ACH occur during or right after emissions, indoor $PM_{2.5}$ concentrations are affected. The different scenarios are illustrated with error bars in Figure 4.

Activities in airtight buildings with windows closed (0.2 ACH) or open before the activity lead to the highest concentrations. In Figure 4(a), we note that there is no uncertainty bar related to scenarios with 0.2 and 0.6 ACH since windows are considered to be closed. In scenarios with

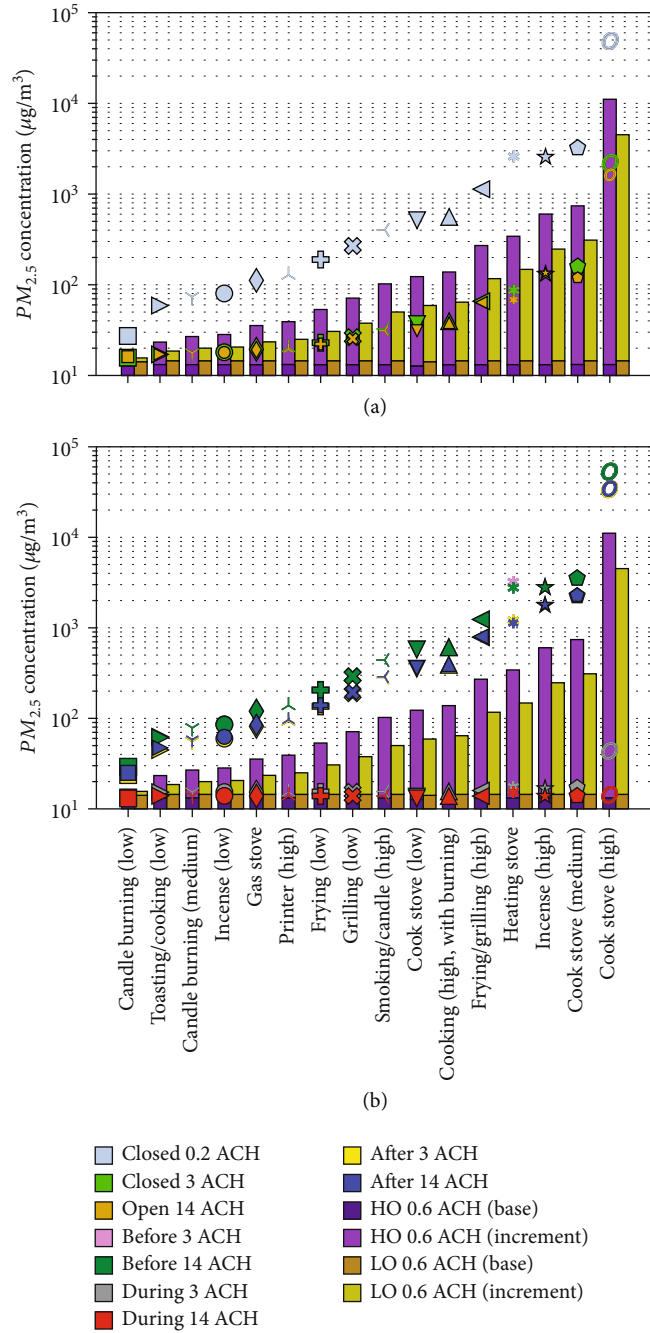


FIGURE 3: Bars represent $PM_{2.5}$ concentrations for an average scenario with 0.6 ACH without indoor emission (base) and with emissions from activities (*increment*) for a room with small volume and high occupancy (HO) and a room with high volume and low occupancy (LO). Markers represent concentrations for (a) three other ACH in the small room: 0.2 ACH (always closed), 3 ACH, and 14 ACH (always open), and (b) two ACH: 3 ACH and 14 ACH for different opening scenarios (open before, open during, and open after).

3 and 14 ACH, windows can be always open or open before, during, or after the activity. Lowest concentrations (lower end of the error bar) correspond to scenarios where windows are open during the emission, evacuating almost all emitted particles and leading to a concentration approximately equal to \bar{C}_{out} . Highest concentrations are linked to windows always being closed, with an infiltration rate of 0.2 ACH or scenarios where the windows are open before

the activity, hence not affecting activity-related concentrations. The uncertainty factors between the parametric model and the dynamic simulation, based on the root mean squared log of error (RMSLE), are 1.18, 1.00, 1.03, and 1.14 for the following scenarios, respectively: closed window at 0.2 ACH and 0.6 ACH and window always open at 3 ACH and 14 ACH. The average percentage error is <3%. The uncertainties are linked to the variations in ACH due to

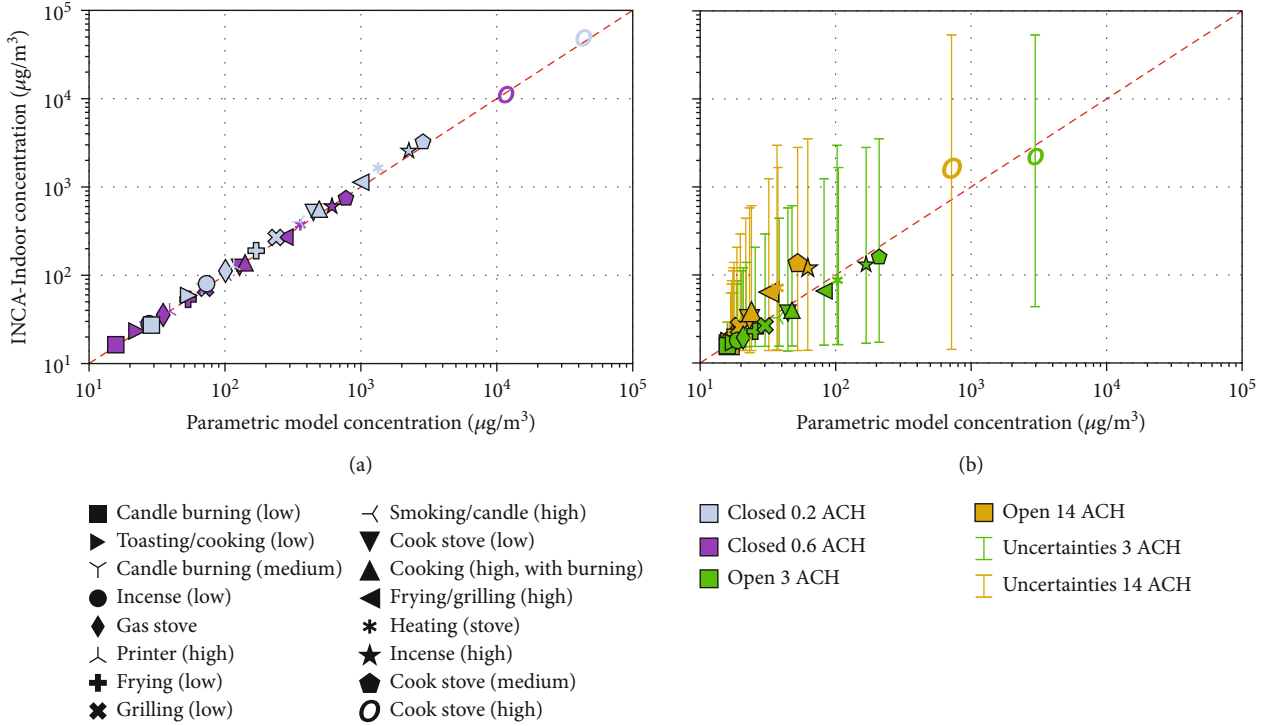


FIGURE 4: INCA-Indoor vs. parametric model 24 h average indoor PM_{2.5} concentrations from different activities for (a) closed windows at 0.2 and 0.6 ACH and (b) air renewal of 3 and 14 ACH for windows always open and uncertainties linked to window-opening scenarios.

meteorological conditions affecting natural ventilation rates, which are not considered by the parametric model (see SI Figure S2).

3.3. Contribution of Outdoor PM_{2.5} Level on Indoor Concentrations. Dynamic and parametric model concentrations were calculated for an average European city with an average background PM_{2.5} level of 16 $\mu\text{g}/\text{m}^3$, while, for different cities in the world, outdoor PM_{2.5} concentrations can range from 4 $\mu\text{g}/\text{m}^3$ to 200 $\mu\text{g}/\text{m}^3$ [45]. Figure 5 illustrates the effect of different outdoor PM_{2.5} levels on indoor concentrations for different ventilation scenarios and three activities representing low, medium, and high emission rates: candle burning (low), frying (low), and cook stove (high).

We note from Figure 5 that, for activities with high emissions such as incense burning, outdoor concentrations have a low relative effect on indoor concentrations (only up to 6% increase), while they can lead to an 8-fold increase for low-emission activities such as candle burning (low). At very high outdoor concentrations and for low emission rates such as candle burning, average concentrations are lower for closed window scenarios since the highest contribution to indoor PM_{2.5} is outdoor air.

3.4. Intake Fractions, Effect Factors, and Characterisation Factors for Different Indoor Activities. Intake quantities and impacts for each activity are calculated per occupant and per hour of activity. The uncertainty factors for the intake mass (μg) calculated by the parametric versus the dynamic model are 1.0, 1.05, 1.04, and 1.37, respectively, for the standard scenarios with 0.2, 0.6, 3, and 14 ACH.

Intake fractions ($\mu\text{g}_{\text{intake}}/\mu\text{g}_{\text{emitted}}$) and intake rates ($\mu\text{g}_{\text{intake}}/\text{h}_{\text{activity}}$) calculated using the dynamic concentrations for all activities and ventilation scenarios are shown in Figure 6(a). Orange and red lines represent the annual and daily exposure recommendations from the WHO air quality guidelines, respectively [8]. Figure 6(b) shows effect factors ($\mu\text{DALY}/\mu\text{g}_{\text{intake}}$) for all activities and four standard ventilation scenarios, and Figure 6(c) shows characterisation factors ($\mu\text{DALY}/\mu\text{g}_{\text{emitted}}$) on the primary y -axis and impact scores ($\mu\text{DALY}/\text{h}_{\text{activity}}$ and $\text{minutes}_{\text{lost}}/\text{h}_{\text{activity}}$) on the secondary y -axes with diagonal iso-impact lines for all activities and scenarios.

Intake fractions ($\mu\text{g}_{\text{intake}}/\mu\text{g}_{\text{emitted}}$) calculated by equation (2) are different for each scenario but independent of the emission rate: they depend on breathing rate, occupancy, particle deposition rate, and ACH [4]. Given a ventilation scenario, the total intake ($\mu\text{g}_{\text{intake}}/\text{h}_{\text{activity}}$), represented by diagonal grey iso-intake lines, is higher for activities with higher emission rates. Markers in the orange and red zone indicate activity and window-opening combinations that lead to concentrations and, consequently, intake quantities, beyond WHO guidelines. These include low-emission activities such as lighting a candle in a closed airtight building at 0.2 ACH, which is a possible scenario. Unless having a very high ventilation rate (windows open only during activity, with a 24 hour average of 14 ACH) during the use of a very high-emission cook stove, all scenarios lead to intake well above guidelines.

Figure 6(b) shows that effect factors decrease with an increasing emission rate for each scenario, since they depend on indoor PM_{2.5} concentrations. Characterisation factors (CF), a product of iF and EF, also vary across activities and

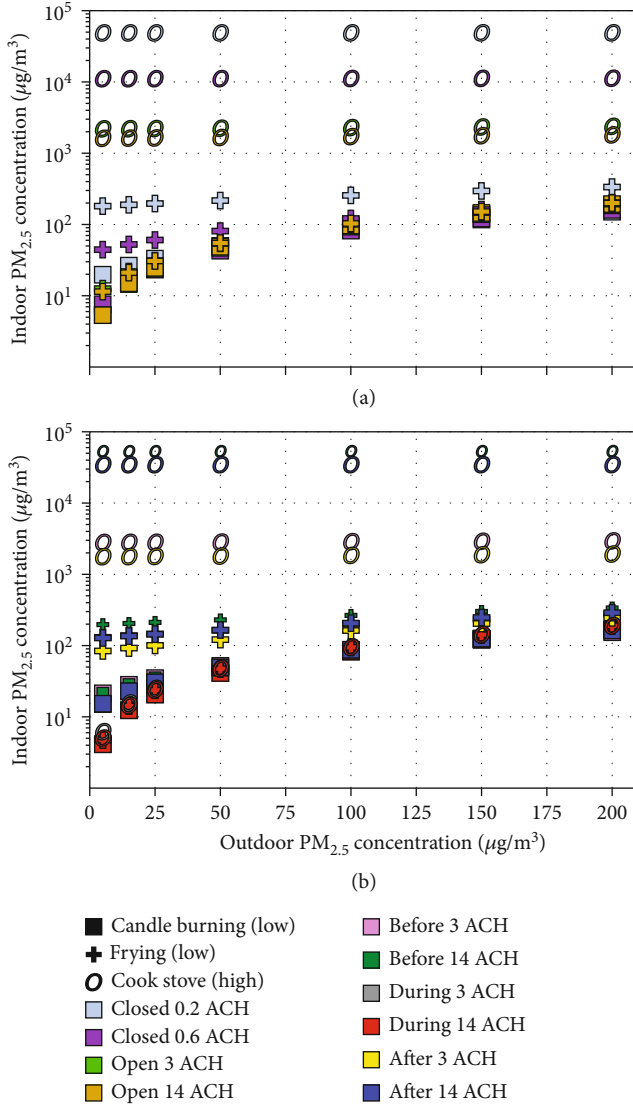


FIGURE 5: Indoor PM_{2.5} concentrations for three different activities and seven outdoor concentrations (4–200 µg/m³) for four standard ACH: (a) 0.2 ACH and 0.6 ACH with closed windows and 3 ACH and 14ACH with windows always open and (b) 3ACH or 14ACH for different opening scenarios (open before, open during, and open after).

scenarios (see Figure 6(c)). Least impacts occur when windows are open during activities, especially if ventilation rates are very high (e.g., with cross-ventilation). We also note that indoor fuel burning for cooking (high, using maize straw) can lead to very high health impacts of 484 µDALY/h_{activity} (about 4 hours_{lost}) in closed buildings at 0.2 ACH. However, these ACH are unlikely for this activity, occurring in rural homes in buildings with potentially high infiltration rates. Furthermore, occupants might ventilate during the use of the cook stove, which can otherwise cause discomfort due to increased temperatures and high, perceptible PM_{2.5} levels. Air renewal rates are more likely to be around 3 to 14 ACH, resulting in 98 to 119 µDALY/h_{activity} (52 to 63 minutes_{lost}/h_{activity}). On the other hand, a candle burning can potentially occur in airtight buildings with closed windows, at

0.2 or 0.6 ACH, leading to 7 to 20 µDALY/h_{activity} (4 to 11 minutes_{lost}/h_{activity}).

For a given activity-window scenario combination in the larger room (67 m³), concentrations are lower (see Figure 3), and impact scores are also lower. Results for the larger room are given in SI.

3.5. Individual Lifetime Risk. The individual lifetime risk (ILR) (DALY/person), representing the number of life years lost from the five disease outcomes, is calculated for each activity for an average scenario of 0.6 ACH air change rate from equation (6) and illustrated in Figure 7. It is considered that an individual is exposed PM_{2.5} resulting from daily one-hour activities over a lifetime of 86 years [46]. The ILR for 30 minute and 2 hour activity durations are also given.

Activities with very high emissions can lead to a loss of up to 10 years of life, distributed as follows for the use of cook stove (high): 42% of the risk is related to IHD, 30% to stroke, 3% to LRI, 9% to LC, and 15% to COPD.

From Figure 7, we note variations in the distance between the ILR for the default activity duration (one hour) and that of each two additional durations (30 minutes and 2 hours) for different activities. These are explained by two nonlinearities, one associated with the effect factor and one associated with the intake. First, the exposure-response model underlying the effect factors is supralinear and dependent on indoor PM_{2.5} concentrations (see equation (3)), which are a function of both indoor activity emissions and outdoor PM_{2.5} levels. Second, intake considers the concentration increment associated with a specific activity and hence is nonlinearly dependent on indoor PM_{2.5} concentrations (especially at very low emission rates, where outdoor PM_{2.5} have a higher relative influence on indoor PM_{2.5} concentrations).

4. Discussion

We have seen that the parametric model can be used with little or no variation in ACH during the day, but cannot integrate dynamic ventilation or occupancy scenarios. As for the dynamic model, window-opening scenarios can be defined with a minimum of one-hour time steps, while in reality, occupants can open windows for only a few minutes, especially during cold weather. Ventilation durations are thus potentially overestimated, leading to underestimations in concentrations and impacts, in particular for the *open during* and *open after* scenarios.

In the particular case of the heating stove, opening windows during the activity is counterproductive, leading to higher heating needs and thus higher environmental impacts. With a life cycle perspective, it is thus important to consider heating as a source of impacts (calculated using an energy simulation and LCA software) and identify best trade-offs that allow the reduction of damage from PM_{2.5} and heating altogether.

The emission factor obtained in the literature is dependent on the mass of coal burnt [21], which was calculated according to heating needs with Pleiades [35]. The emission rate could thus be adapted in the model if specific

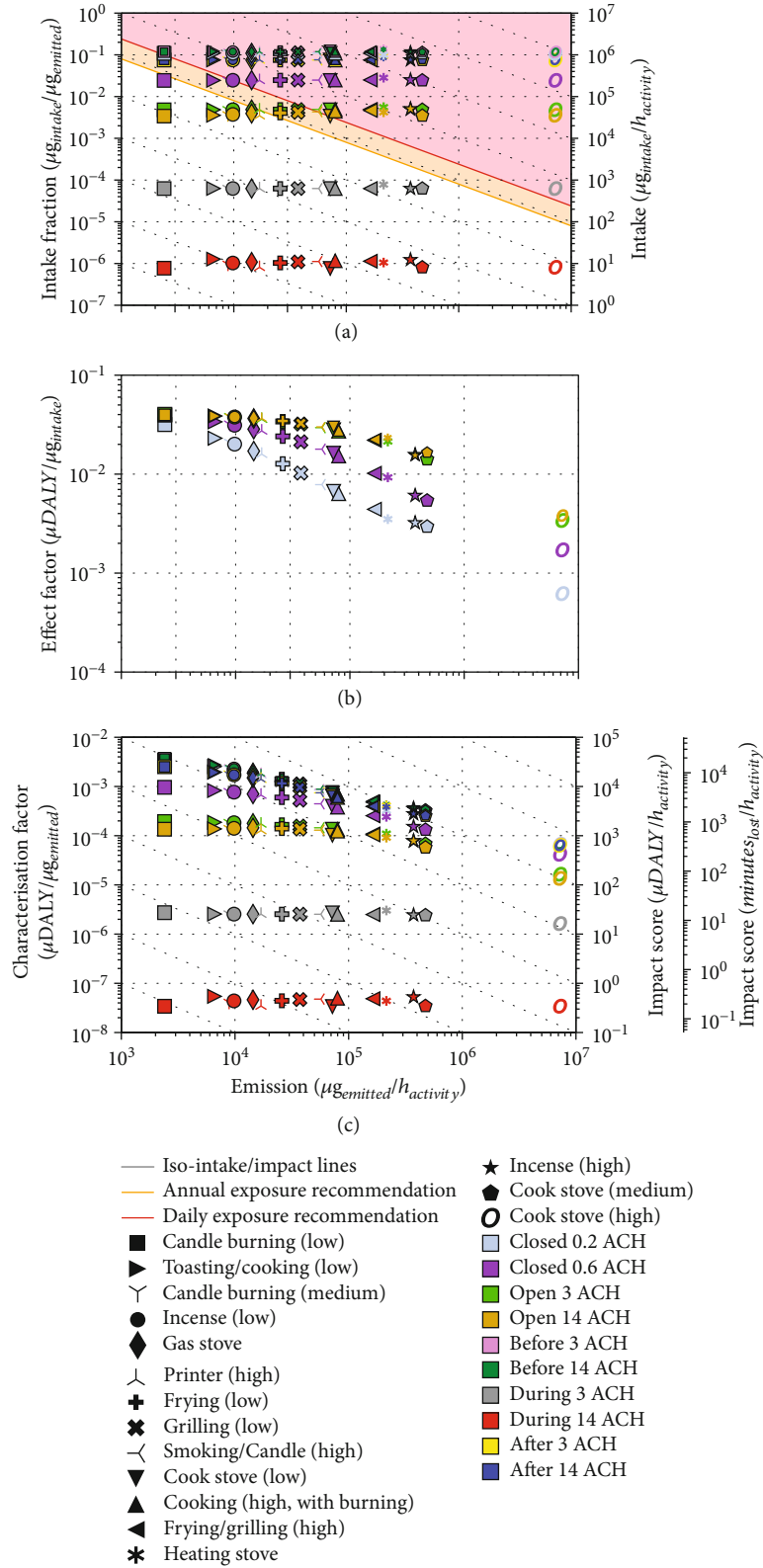


FIGURE 6: (a) Intake fractions ($\mu\text{g}_{\text{intake}}/\mu\text{g}_{\text{emitted}}$) for all activities and ventilation scenarios on the primary y -axis and total intake ($\mu\text{g}_{\text{intake}}/h_{\text{activity}}$) on the secondary y -axis, with iso-intake diagonal lines in grey and annual and daily recommendations represented by yellow and red lines, respectively; (b) effect factors ($\mu\text{DALY}/\mu\text{g}_{\text{intake}}$) for all activities and four standard ventilation scenarios; and (c) characterisation factors ($\mu\text{DALY}/\mu\text{g}_{\text{emitted}}$) on the primary y -axis and health damages ($\mu\text{DALY}/h_{\text{activity}}$ and $\text{minutes}_{\text{lost}}/\text{d}$) on the two secondary y -axes (left and right) with iso-impact diagonal lines in grey.

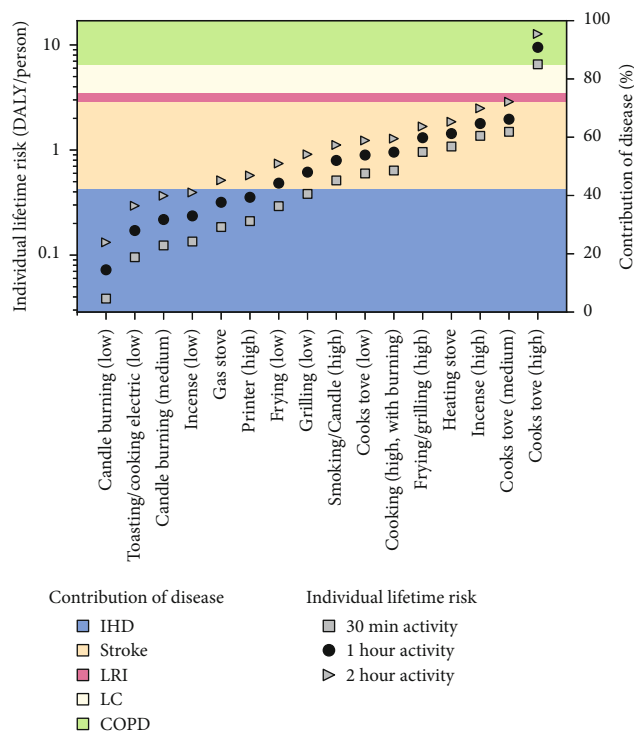


FIGURE 7: Total individual lifetime risks (DALY/person) given by black markers for 1 hour activities at 0.6 ACH and grey markers for 30 minute and 2 hour durations on the left y-axis, with contributions of each disease (ischaemic heart disease (IHD), stroke, lower respiratory infections (LRI), lung cancer (LC), and chronic obstructive pulmonary disease (COPD)) given on the right y-axis.

information on the mass burnt or the heating need is known. Furthermore, activities linked with the indoor burning of fuels are more likely to occur in rural regions, in homes having high ventilation/infiltration rates. Different ventilation rates can be used as sensitivity analysis to reflect associations between indoor pollution levels and occupant behaviour (e.g., opening of windows when concentrations are uncomfortably high), especially if actual ventilation rates are unknown. In an LCA context, results are given for a large number of scenarios that combine different emission rates and building characteristics (i.e., ventilation rates and occupancy). Practitioners can thus apply those results that are relevant for their specific study context.

Health impacts are calculated for activities with a reference duration of one hour, but some activities can be shorter (e.g., smoking for a few minutes) or last longer (e.g., heating for a few hours). Scaling results to actual activity durations can provide approximations, since the calculated nonlinear effect factors depend on average indoor air $PM_{2.5}$ concentrations, which vary with different activity durations. A sensitivity analysis is given in SI section S.6 for the duration of 30 minutes and 2 hours for all activities at 0.6 ACH. Similarly, the factors provided do not consider multiple occurrences of different activities at the same time, which could increase concentrations and lead to variations in effect factors and impact scores. Finally, the emission of other contaminants from the activities (e.g., volatile organic compounds, VOCs, and from candle

burning) was not considered, which could be responsible for additional health impacts.

Future scopes include the study of the influence of PM toxicity if compositions of emitted particles for specific activities are known, and the calculation of characterisation factors and impact scores for more activities. Studies focusing on fugitive emissions are few and fairly recent. With growing awareness around health impacts of indoor solid fuel burning for heating or cooking, more data could be available and allow the derivation of impact scores for different types of stoves (e.g., certified heating stoves). The effect of a kitchen hood, which leads to 60 to 100% reduction in $PM_{2.5}$ concentrations [47], on health impacts of cooking could be included. Furthermore, effect factors were calculated based on ambient $PM_{2.5}$ concentrations, though occupants are mainly exposed to indoor concentrations, which are often higher than those outdoors: effect factors are hence possibly overestimated. Representative building archetypes with their respective activity scenarios can be modelled to calculate annual exposure concentrations considering the fractions of time spent indoors and outdoors.

5. Conclusion

In this paper, we have provided a set of intake fractions, effect factors, characterisation factors, and impact scores for 19 one-hour activities and 10 different ventilation scenarios. Indoor concentrations depend on indoor settings (e.g., window layout and opening scenarios), outdoor $PM_{2.5}$ level, and activity duration. These parameters influence the indoor exposure $PM_{2.5}$ level used to calculate effect factors. We note that, at very low ACH, all activities induced exposure concentrations beyond WHO recommendations. High or very high ventilation *during* all activities allowed the reduction of concentrations well below these recommendations. For instance, 98 to 119 $\mu\text{DALY}/h_{\text{activity}}$ (52 to 63 minutes_{lost}/ h_{activity}) was associated with traditional fuel cook stoves, with high air renewal rates (3 and 14 ACH), while 7 to 11 $\mu\text{DALY}/h_{\text{activity}}$ (4 to 11 minutes_{lost}/ h_{activity}) was associated with candle burning in closed buildings at 0.2 to 0.6 ACH. Characterisation factors for the one-hour activities (or any other activities with corresponding emission rates) provided in this study can be integrated to LCIA methods, and the framework proposed can help to devise optimal ventilation strategies in building design. The derived impact scores ($CF \times ER_{\text{activity}}$) for an activity unit of one hour can be scaled by activity duration to obtain an approximation of actual activity impacts. This constitutes a valuable starting point for the integration of indoor activities and their $PM_{2.5}$ -related emissions, exposures, and health effects into LCA and environmental footprint studies.

Data Availability

Data are available upon request from the first author.

Conflicts of Interest

The authors declare that they have no conflicts of interest.

Acknowledgments

The authors are thankful for the financial support of the PhD thesis by the Chair ParisTech VINCI Eco-design of buildings and infrastructure. The project acknowledges the UNEP GLAM human health task force and the financial support from the USEtox International Centre.

Supplementary Materials

Supplementary 1. Background model data, ventilation scenario descriptions, heat stove emission calculations, particle size number distribution, indoor PM_{2.5} concentrations as a function of the ventilation scenario, and results for the larger room are provided.

Supplementary 2. Effect factors, characterisation factors, and impact scores for all activities, scenarios, and occupancy rates are given.

References

- [1] C. J. L. Murray, A. Y. Aravkin, P. Zheng et al., “Global burden of 87 risk factors in 204 countries and territories, 1990–2019: a systematic analysis for the Global Burden of Disease Study 2019,” *The Lancet*, vol. 396, no. 10258, pp. 1223–1249, 2020.
- [2] R. T. Burnett, C. A. Pope, M. Ezzati et al., “An integrated risk function for estimating the global burden of disease attributable to ambient fine particulate matter exposure,” *Environmental Health Perspectives*, vol. 122, no. 4, pp. 397–403, 2014.
- [3] P. Fantke, O. Jolliet, J. S. Evans et al., “Health effects of fine particulate matter in life cycle impact assessment: findings from the Basel Guidance Workshop,” *International Journal of Life Cycle Assessment*, vol. 20, no. 2, pp. 276–288, 2015.
- [4] P. Fantke, O. Jolliet, J. S. Apte et al., “Characterizing aggregated exposure to primary particulate matter: recommended intake fractions for indoor and outdoor sources,” *Environmental Science & Technology*, vol. 51, no. 16, pp. 9089–90100, 2017.
- [5] Observatoire de la Qualité de l’Air Intérieur, “Une campagne nationale pour évaluer la qualité des environnements intérieurs des écoles françaises 2018,” <http://www.oqai.fr/fr/campagnes/campagne-nationale-ecoles-n01>.
- [6] C. Mandin, “The indoor air quality observatory (OQAI): a unique project to understand air pollution in our living spaces,” *Field Actions Science Reports The Journal of Field Actions*, vol. 21, pp. 18–23, 2020.
- [7] A. Mainka and P. Fantke, “Preschool children health impacts from indoor exposure to PM2.5 and metals,” *Environment International*, vol. 160, article 107062, 2022.
- [8] World Health Organization, *WHO global air quality guidelines: particulate matter (PM2.5 and PM10), ozone, nitrogen dioxide, sulfur dioxide and carbon monoxide*, World Health Organization, 2021.
- [9] K. R. Smith, “National burden of disease in India from indoor air pollution,” *Proceedings of the National Academy of Sciences*, vol. 97, no. 24, pp. 13286–13293, 2000.
- [10] K. R. Smith, J. P. McCracken, M. W. Weber et al., “Effect of reduction in household air pollution on childhood pneumonia in Guatemala (RESPIRE): a randomised controlled trial,” *The Lancet*, vol. 378, no. 9804, pp. 1717–1726, 2011.
- [11] H. Rohra, R. Tiwari, N. Khandelwal, and A. Taneja, “Mass distribution and health risk assessment of size segregated particulate in varied indoor microenvironments of Agra, India - a case study,” *Urban Climate*, vol. 24, pp. 139–152, 2018.
- [12] D. Srivastava, T. V. Vu, S. Tong, Z. Shi, and R. M. Harrison, “Formation of secondary organic aerosols from anthropogenic precursors in laboratory studies,” *NPJ Climate and Atmospheric Science*, vol. 5, no. 1, pp. 1–30, 2022.
- [13] J. Pagels, A. Wierzbicka, E. Nilsson et al., “Chemical composition and mass emission factors of candle smoke particles,” *Journal of Aerosol Science*, vol. 40, no. 3, pp. 193–208, 2009.
- [14] N. J. Aquilina and S. F. Camilleri, “Impact of daily household activities on indoor PM_{2.5} and black carbon concentrations in Malta,” *Building and Environment*, vol. 207, article 108422, 2022.
- [15] C. M. Long, H. H. Suh, and P. Koutrakis, “Characterization of indoor particle sources using continuous mass and size monitors,” *Journal of the Air & Waste Management Association*, vol. 50, no. 7, pp. 1236–1250, 2000.
- [16] C. He, L. Morawska, J. Hitchins, and D. Gilbert, “Contribution from indoor sources to particle number and mass concentrations in residential houses,” *Atmospheric Environment*, vol. 38, no. 21, pp. 3405–3415, 2004.
- [17] J. Tissari, J. Lyyränen, K. Hytönen et al., “Fine particle and gaseous emissions from normal and smouldering wood combustion in a conventional masonry heater,” *Atmospheric Environment*, vol. 42, no. 34, pp. 7862–7873, 2008.
- [18] G. Shen, W. Du, Z. Luo et al., “Fugitive emissions of CO and PM2.5 from indoor biomass burning in chimney stoves based on a newly developed carbon balance approach,” *Environmental Science & Technology Letters*, vol. 7, no. 3, pp. 128–134, 2020.
- [19] I. Demanega, I. Mujan, B. C. Singer, A. S. Anđelković, F. Babich, and D. Licina, “Performance assessment of low-cost environmental monitors and single sensors under variable indoor air quality and thermal conditions,” *Building and Environment*, vol. 187, article 107415, 2021.
- [20] W. Du, S. Zhuo, J. Wang et al., “Substantial leakage into indoor air from on-site solid fuel combustion in chimney stoves,” *Environmental Pollution*, vol. 291, article 118138, 2021.
- [21] C. Li, K. Ye, W. Zhang et al., “User behavior, influence factors, and impacts on real-world pollutant emissions from the household heating stoves in rural China,” *Science of the Total Environment*, vol. 823, article 153718, 2022.
- [22] A. R. Ferro, R. J. Kopperud, and L. M. Hildemann, “Source strengths for indoor human activities that resuspend particulate matter,” *Environmental Science & Technology*, vol. 38, no. 6, pp. 1759–1764, 2004.
- [23] R. L. Corsi, J. A. Siegel, and C. Chiang, “Particle resuspension during the use of vacuum cleaners on residential carpet,” *Journal of Occupational and Environmental Hygiene*, vol. 5, no. 4, pp. 232–238, 2008.
- [24] S. Bhangar, R. I. Adams, W. Pasut et al., “Chamber bioaerosol study: human emissions of size-resolved fluorescent biological aerosol particles,” *Indoor Air*, vol. 26, no. 2, pp. 193–206, 2016.
- [25] D. Licina, Y. Tian, and W. W. Nazaroff, “Emission rates and the personal cloud effect associated with particle release from the perihuman environment,” *Indoor Air*, vol. 27, no. 4, pp. 791–802, 2017.
- [26] D. Al Assaad, K. Ghali, N. Ghaddar, and E. Shammas, “Modeling of indoor particulate matter deposition to occupant typical wrinkled shirt surface,” *Building and Environment*, vol. 179, article 106965, 2020.

- [27] P. Fantke, W. A. Chiu, L. Aylward et al., "Exposure and toxicity characterization of chemical emissions and chemicals in products: Global recommendations and implementation in USEtox," *International Journal of Life Cycle Assessment*, vol. 26, pp. 899–915, 2021.
- [28] N. Hodas, M. Loh, H.-M. Shin et al., "Indoor inhalation intake fractions of fine particulate matter: review of influencing factors," *Indoor Air*, vol. 26, no. 6, pp. 836–856, 2016.
- [29] M. Mendez, N. Blond, P. Blondeau, C. Schoemaeker, and D. A. Hauglustaine, "Assessment of the impact of oxidation processes on indoor air pollution using the new time-resolved INCA-Indoor model," *Atmospheric Environment*, vol. 122, pp. 521–530, 2015.
- [30] S. Humbert, J. D. Marshall, S. Shaked et al., "Intake fraction for particulate matter: recommendations for life cycle impact assessment," *Environmental Science & Technology*, vol. 45, no. 11, pp. 4808–4816, 2011.
- [31] A. J. Cohen, M. Brauer, R. Burnett et al., "Estimates and 25-year trends of the global burden of disease attributable to ambient air pollution: an analysis of data from the Global Burden of Diseases Study 2015," *The Lancet*, vol. 389, no. 10082, pp. 1907–1918, 2017.
- [32] P. Fantke, T. E. McKone, M. Tainio et al., "Global effect factors for exposure to fine particulate matter," *Environmental Science & Technology*, vol. 53, no. 12, pp. 6855–6868, 2019.
- [33] S.-C. Lee and B. Wang, "Characteristics of emissions of air pollutants from burning of incense in a large environmental chamber," *Atmospheric Environment*, vol. 38, no. 7, pp. 941–951, 2004.
- [34] C. He, L. Morawska, H. Wang et al., "Quantification of the relationship between fuser roller temperature and laser printer emissions," *Journal of Aerosol Science*, vol. 41, no. 6, pp. 523–530, 2010.
- [35] Izuba Énergies, *Logiciel Pleiades*, IZUBA ÉNERGIES, 2001, <http://www.izuba.fr/logiciels/outils-logiciels/>.
- [36] J. D. Biesebeek, M. M. Nijkamp, B. G. H. Bokkers, and S. W. P. Wijnhoven, *Room size and ventilation. General fact sheet: general default parameters for estimating consumer exposure: updated version 2014*, National Institute for Public Health and the Environment, 2014.
- [37] P. F. Pereira, N. M. M. Ramos, and A. Ferreira, "Room-scale analysis of spatial and human factors affecting indoor environmental quality in Porto residential flats," *Building and Environment*, vol. 186, article 107376, 2020.
- [38] P. Kumar, S. Hama, R. A. Abbass et al., "CO₂ exposure, ventilation, thermal comfort and health risks in low-income home kitchens of twelve global cities," *Journal of Building Engineering*, vol. 61, article 105254, 2022.
- [39] E. Abt, H. H. Suh, P. Catalano, and P. Koutrakis, "Relative contribution of outdoor and indoor particle sources to indoor concentrations," *Environmental Science & Technology*, vol. 34, no. 17, pp. 3579–3587, 2000.
- [40] R. K. Rosenbaum, A. Meijer, E. Demou et al., "Indoor air pollutant exposure for life cycle assessment: regional health impact factors for households," *Environmental Science & Technology*, vol. 49, no. 21, pp. 12823–12831, 2015.
- [41] A. Persily, A. Musser, and S. J. Emmerich, "Modeled infiltration rate distributions for U.S. housing," *Indoor Air*, vol. 20, no. 6, pp. 473–485, 2010.
- [42] R. Aynsley, "Indoor wind speed coefficients for estimating summer comfort," *International Journal of Ventilation*, vol. 5, no. 1, pp. 3–12, 2006.
- [43] United Nations, "Department of Economic and Social Affairs, Population Division," in *World urbanization prospects: the 2018 revision*, UN, 2019.
- [44] GBD Global Burden of Disease Collaborative Network, *Global Burden of Disease study 2019 (GBD 2019) results*, Institute for Health Metrics and Evaluation, 2019, <http://healthdata.org/gbd-results>.
- [45] World Health Organization, *Modelled estimates of air pollution from particulate matter 2016* <http://www.who.int/data/gho/data/themes/air-pollution/who-modelled-estimates-of-air-pollution-from-particulate-matter>.
- [46] World Health Organization, *WHO methods and data sources for global burden of disease estimates 2000-2019 2020* https://cdn.who.int/media/docs/default-source/gho-documents/global-health-estimates/ghe2019_daly-methods.pdf?sfvrsn=31b25009_7.
- [47] Y. S. Eom, D. H. Kang, D. Rim, and M. Yeo, "Particle dispersion and removal associated with kitchen range hood and whole house ventilation system," *Building and Environment*, vol. 230, article 109986, 2023.